Int. J. Nanosci. Nanotechnol., Vol. 20, No. 1, March 2024, pp. 63-76
DOI: 10.22034/ijnn.2024.531286.2050

***Short Communication***

# Study on Degradation of Textile Dyes by Photocatalytic Ozonation Assisted with Tin Doped Zinc Oxide Nanorods

**R. Rajeswari[1,*] and G. Poongodi[2]**

[1]Department of Chemistry, Quaid-E-Millath Govt. College for Women, Chennai - 600 002
[2]Department of Physics, Quaid-E-Millath Govt. College for Women, Chennai - 600 002

(*) Corresponding author: rajiraja99@gmail.com

*(Received: 29 May 2021 and Accepted: 16 November 2023)*

***Abstract***

*The current research work focuses on the synergistic effect of tin doped Zinc oxide(Sn- ZnO) nanorods in combination with ozonation for the degradation of dyes in the water released from textile industries. Well crystalline mono dispersed Sn doped ZnO (Sn-ZnO) nanorods have been synthesized by simple hydrothermal method. The XRD results show the hexagonal wurtzite structure of the prepared catalyst. The result of EDAX and XPS revealed that Sn was doped in to ZnO lattices. FESEM image show that the sample possesses hexagonal rod morphology with an average of 1µm in length and 50 to 100nm in diameter. Optical transmittance of the sample was recorded in the wavelength range of 300–800 nm, and the band gap was determined. The prepared nanocatalyst in combination with ozone is used for the photocatalytic ozonation (nano PCO) of the azo dyes taken for the present study. Nano PCO is carried out in a laboratory scale photocatalytic ozonation reactor. The experiments were conducted under different ozone dosages (0.12-0.57 g/h), pH (3-9), catalyst dosage (0-2 g/L) and dye concentration (5-50 mg/L) to arrive at optimized reaction conditions for degradation of dyes by Sn-ZnO assisted PCO. Three experimental sets (Sn-ZnO/UV, UV/$O_3$ and Sn-ZnO/UV/$O_3$) were carried out under optimized reaction conditions to prove the synergistic effect of ozone on Sn-ZnO. Use of ozone with Sn-ZnO leads to 95% decolourisation of the dyes in 30 min and 79.4% mineralization in 180 min. The reusability of the photocatalyst was checked six times and the results revealed that the efficiency of the sample slightly decreased at the end of sixth cycle. Based on the above results, the current route is promising for the application of Sn-ZnO based nanocatalyst in combination with ozonation for wastewater treatment.*

***Keywords:*** *Sn doped ZnO (Sn-ZnO), Photocatalytic Ozonation (PCO), Azo dyes, Synergistic effect.*

## 1. INRODUCTION

Water polluted with dyes constitutes an increasing environmental pollutant, mainly in places such as India, where textile industries play a vital role in the economic growth. During the last decade, the unregulated discharge of textile effluents by the industries into the water bodies have had much more deleterious effects on our environment, than the benefits it bestowed to the society. Due to the recalcitrant chemical nature of dyes, photochemical, chemical and bio-chemical degradation of wastewater is much limited.

The current wastewater treatment methods adopted in industries are solar evaporation or biological treatment systems which are not effective in elimination of these different classes of dyes. In the last decade, a lot of research has been addressed to a special class of oxidation technique known as Advanced Oxidation Processes (AOPs), pointing out its prospective major role in the wastewater treatment [1-7]. These treatment processes are considered as very promising methods for the remediation of ground and surface waters that are polluted by non-biodegradable, toxic organic industrial effluents. In particular, semiconductor mediated nano photo-catalysis is a rapidly developing field of research with a wide range of applications in water disinfection, hazardous waste remediation and water purification. Among various photocatalysts, Zinc Oxide (ZnO) with high surface reactivity owing to large number of active sites and other innate characteristic has emerged as an efficient photocatalyst. It absorbs wider spectrum of radiation and has high photochemical reactivity. It can be synthesized under mild conditions and various methods have been adopted. Electrochemical deposition method is used for production of zinc oxide nanorods [8]. Various sizes of ZnO nanoparticles are synthesized for the study on degradation of dyes by sol-gel method [9]. Amongst the various synthesizing routes of nanoparticles, hydrothermal method has gained great success in producing nanaomaterials as it has low energy consumption, normal operating conditions and environmentally benign. Low operating temperatures, diversified morphologies and pronounced crystallinity of the nanoparticles along with high purity makes this process more advantages than other methods [10]. This method is expected to produce nanorods with minimal defects, good homogeneity having special morphology and metastable phase thermodynamics [11].

However, the rapid recombination rate of the photo induced charge carriers in ZnO results in reduction of its photocatalytic activity which is unfavourable for commercial application [12, 13]. One of the important strategies to reduce the recombination of charge carriers in ZnO is doping where doping generates more defects and vacancies which traps the charge carriers and enhances photocatalytic activity of ZnO [14-16]. Recent studies demonstrated that transition metal doping into ZnO lattices can tune various properties of ZnO and enhance its visible light photocatalytic activity [17-21]. Many efforts have been taken to prepare different morphology of doped ZnO nanoparticles. Some of the methods used co-precipitation [22, 23]. Pulsed laser deposition [24] and vapour phase transport [25]. Many elements have been identified for doping with ZnO [26]. Aluminium doped ZnO [27] is used for the study on degradation kinetics for photocatalytic reaction of methyl orange. Yarahmadi et. al., [28] have synthesized Strontium doped ZnO nanoparticles for photocatalytic applications. Cadmium doped ZnO nanocatalyst is used for degradation of textile dyeing wastewater [29]. Siva et al [30] have synthesized and characterized Sn doped ZnO nanoparticles and studied the optical and photocatalytic behaviour with model dye methylene blue. Among them, Sn is considered as an important dopant material for ZnO, because of the different structure of the electronic shell and the similar ionic radii of $Sn^{4+}$ (0.071nm) and $Zn^{2+}$ (0.074nm) [31]. The incorporation of Sn in ZnO lattice generates reactive oxidant species, when it is illuminated by UV or visible light that in turn enhances the photocatalytic activity of the sample. Furthermore, one dimensional (1D) nanostructures such as nanorods, nanofibers and nanowires also improves the photocatalytic activities of ZnO since electrons are confined in one dimension (1D).

However, as the number and concentration of contaminants increase, the process becomes more complicated and challenging problems such as catalyst deactivation, slow kinetics, low photo efficiency and unpredictable mechanism need to be solved. Despite the great efforts devoted to the study of photocatalytic processes, only few studies have been found in the literature of their application on industrial scale. Although total elimination of the active species can be achieved in most cases, complete mineralization of organic matter usually requires longer periods of treatment.

In order to improve the performance of photocatalytic process, different strategies have been used. On the other hand, the use of ozone for the destruction of organics in water is considered as a well-known water treatment technique. $O_3$ is a powerful oxidant ($E^\circ$ =2.07V) and reacts with many compounds via direct or indirect reactions. Indirectly, $O_3$ can react through hydroxyl radical ($E^\circ$=2.8V) which is a powerful and nonselective oxidant and can react with almost all organic compounds [32, 33].

The similarity between the mechanisms of destruction in AOPs indicates that appropriate combination of these oxidation systems could give better performance, as compared to individual processes and some of the drawbacks of one process could be eliminated by some characteristics of other processes. The efficacy of these processes depends strongly on the rate of generation of the free radicals and their utilization by organic molecules.

Photocatalytic ozonation (PCO) is one such emerging new technology which uses the combination of photocatalysis and ozonation. It has been recently studied in treating dibutyl phthalate [34], oxalate ions [35], carboxylic acids [36], phenolic [37] and pesticide wastewaters [38]. Further, a review on different compounds degraded by PCO has been published [39] and the results showed that the combination of two methods manifested the removal of organics in effluent in shorter period.

The present work reports the degradation of textile dyeing wastewater by PCO assisted by Sn-ZnO nanorods. Sn-ZnO nanorods were synthesized by a simple hydrothermal method and the effect of varying experimental parameters such as pH, Ozone dosage, dye concentration and Catalyst dosage was investigated. Azo dyes such as Reactive Red 120 (RR 120), Reactive Yellow 145 (RY145) and Amaranth have been taken as model dye pollutants for the present study. The synergistic effect of ozonation on Sn-ZnO photocatalysis was evaluated and compared with individual techniques.

## 2. MATERIALS AND METHODS

### 2.1 Materials

Azo group of dyes such as RY 145, Amaranth and RR 120 were selected as model dyes which are prevalently present in textile effluents. $ZnCl_2$ and $SnCl_4$ were used without any further preliminary treatment. All the other chemicals such as hexamethylene tetramine, KI, $Na_2S_2O_3$ $5H_2O$, $NH_4OH$, $H_2SO_4$ and NaOH are 98% pure and are supplied by Merck which are analytical grade. All the aqueous solutions are prepared with double distilled water.

### 2.2 Preparation of Sn Doped ZnO Nanorods

Sn-ZnO nanocatalyst was prepared by hydrothermal method. Aqueous solutions of 0.1M $ZnCl_2$ and 0.01M $SnCl_4$ were mixed under continuous stirring for 45 min at room temperature. After stirring, aqueous solution of 0.1M hexamethylene-etetramine was added and stirred for 30 min. The pH of the solution was maintained at 8 by adding few drops of $NH_4OH$. The final solution was again vigorously stirred for 30 min and transferred to Teflon lined autoclave which was then sealed and heated up to120°C for 5 h. The same procedure was repeated without $SnCl_4$ for pure ZnO. After terminating the reaction, the autoclave was allowed to cool at room-temperature and the obtained products were washed several times with deionised water and ethanol. Finally the prepared products were dried at 60°C. The catalyst thus prepared is used for the degradation of azo dyes in an annular photocatalytic ozonation reactor.

### 2.3 Photocatalytic Ozonation with Prepared Sn Doped ZnO Nanorods

For the experimental runs, a pyrex annular photoreactor as shown in Figure 1 has been used. The photoreactor containing 500mL of aqueous suspension was provided with ports in the upper part for inlet and outlet of ozone and at the lower part to withdraw aliquots of reacting suspension.

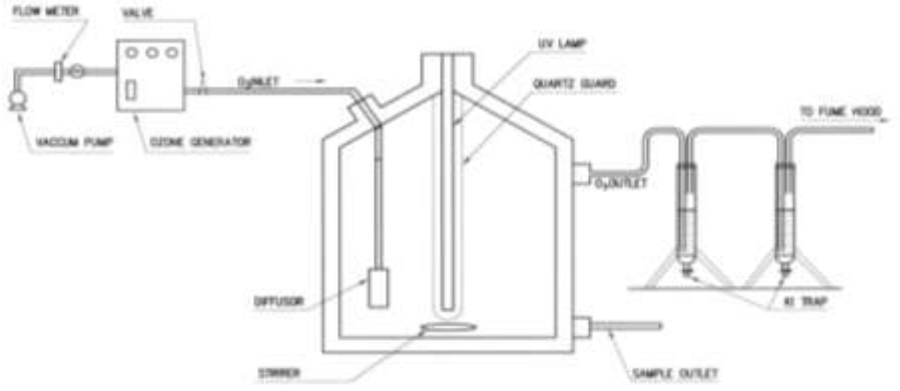

***Figure 1.*** *Reactor set up for Photocatalytic ozonation.*

A medium pressure mercury lamp of 15W was immersed in axial position inside the photoreactor. The photon flux emitted by the lamp has its maximum value at 365 nm. Sn-ZnO was used as photocatalyst without any further preliminary treatment. 0.2 g/L of photocatalyst was added to 500 mL of the dye solution (20 mg/L). Ozone was generated by feeding synthetic air to the Ozone generator (Indiozone, India) and was able to vary the $O_3$ production rate in 0.12g/h to 0.54 g/h range. The initial pH was adjusted using 0.1N $H_2SO_4$ or 0.1N NaOH. The temperature of the suspension was maintained at 20±1° C. The slurry mixed by magnetic stirrer was allowed to attain steady state in the dark for 30 min. after which Ozone was passed through the reactor. Aliquots of samples were withdrawn at specified intervals of time. The reaction parameters such as ozone dosage, pH, catalyst dosage and dye concentration were optimized and final degradation experiment was performed in the annular reactor with optimized reaction conditions. Samples were withdrawn at regular intervals and analysed for the percentage of decolourisation and degradation. Decolourisation was monitored by decrease in absorbance at 418nm, 522nm and 530 nm respectively for RY145, Amaranth and RR120 in the UV-visible spectrophotometer. Chemical Oxygen Demand measured by open reflux potassium dichromate titrimetric method [40] showed the decrease in degradation. TOC was measured using Total Organic Carbon Analyser.

## 3. CHARACTERIZATION

The pure and Sn-ZnO samples were investigated by XRD using Rigaku Minflex-IIC model diffractometer with CuK$_\alpha$ radiation ($\lambda$ = 1.5406Å) in the scan range (2$\theta$) from 20° to 80° at room temperature. The surface morphology and elemental confirmation of the Sn-ZnO sample was studied using FEI Quanta FEG 200 model FESEM operated at 30 kV equipped with an energy-dispersive X-ray (EDAX) detector. X-ray photoelectron spectroscopy (XPS) analysis was carried out to determine the chemical states of the elements present in the sample. The optical transmission spectra were recorded using LABINDIA T90+ UV-Vis spectrophotometer in the wavelength range of 300-800 nm.

## 4. RESULTS AND DISCUSSION

### 4.1 Structural Studies

The powder XRD patterns of the pure and Sn-ZnO samples are depicted in Figure 2. The XRD results reveal that the samples are in single crystalline phase with hexagonal wurtzite structure. Within the

XRD detection limit, no extra diffraction peak from Sn related a second phase was observed. This indicates that $Sn^{4+}$ substituted for $Zn^{2+}$ of ZnO host without changing the wurtzite structure.

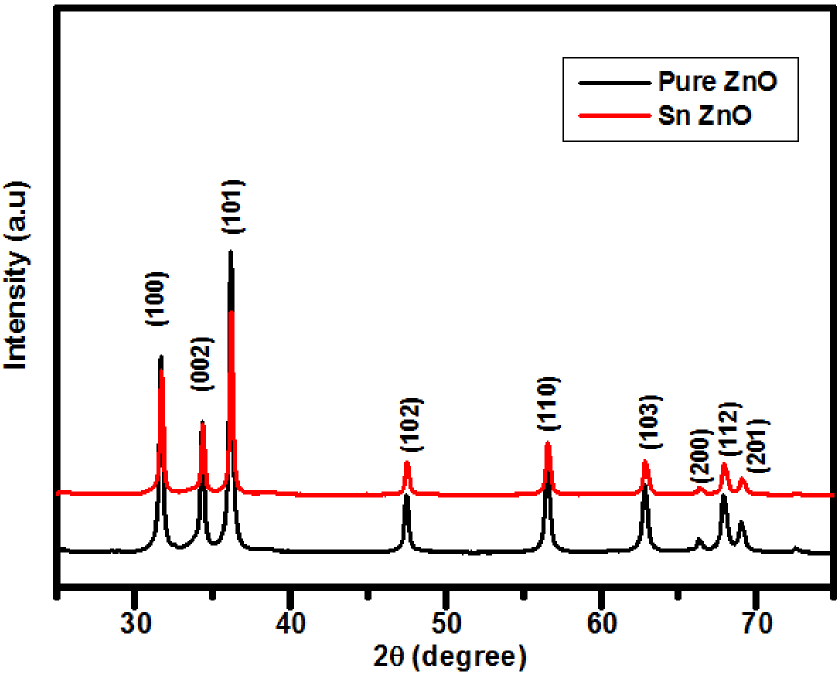

***Figure 2.*** *Powder XRD patterns of Pure and Sn-ZnO nanorods.*

The intensity of the (1 0 1) plane in the pure ZnO is much stronger than that of Sn doped ZnO and a slight shift of peaks positions related to the change of lattice spacing was observed due to the substitution of relatively less ionic radii (0.071 nm) $Sn^{4+}$ at the $Zn^{2+}$ (0.074 nm) sites. The weak intensity peaks and the slight shift of peaks positions may imply that $Sn^{4+}$ incorporates into the ZnO lattices and substitutes the $Zn^{2+}$ site.

### 4.2 Morphological and Compositional Analysis

The surface morphology and compositional analysis of Sn-ZnO sample was determined using field emission scanning electron microscopy (FE-SEM) equipped with EDAX analysis. FESEM image reveals that the sample consists of nanorods with length and diameter in the order of 1µm and 50-90 nm.

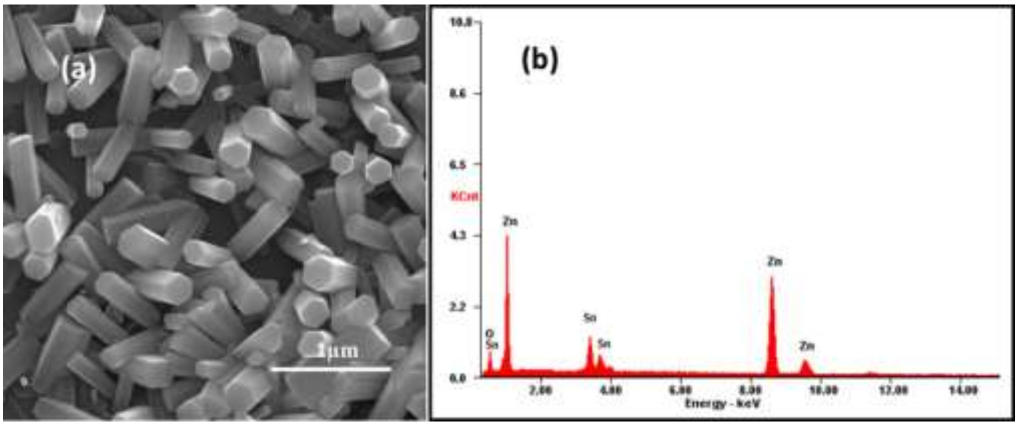

***Figure 3.*** *(a) FESEM image of Sn doped ZnO (b) EDAX spectrum of Sn-ZnO.*

Figure 3(a) indicates the uniform distribution of hexagonal nanorods without any defects and exhibit good crystalline quality. The EDAX analysis was performed to confirm the presence of Sn in ZnO. Figure 3(b) show the EDAX spectrum of Sn-ZnO sample. The results reveal that the sample consists of Zn, Sn and O which confirms the substitution of Sn in ZnO.

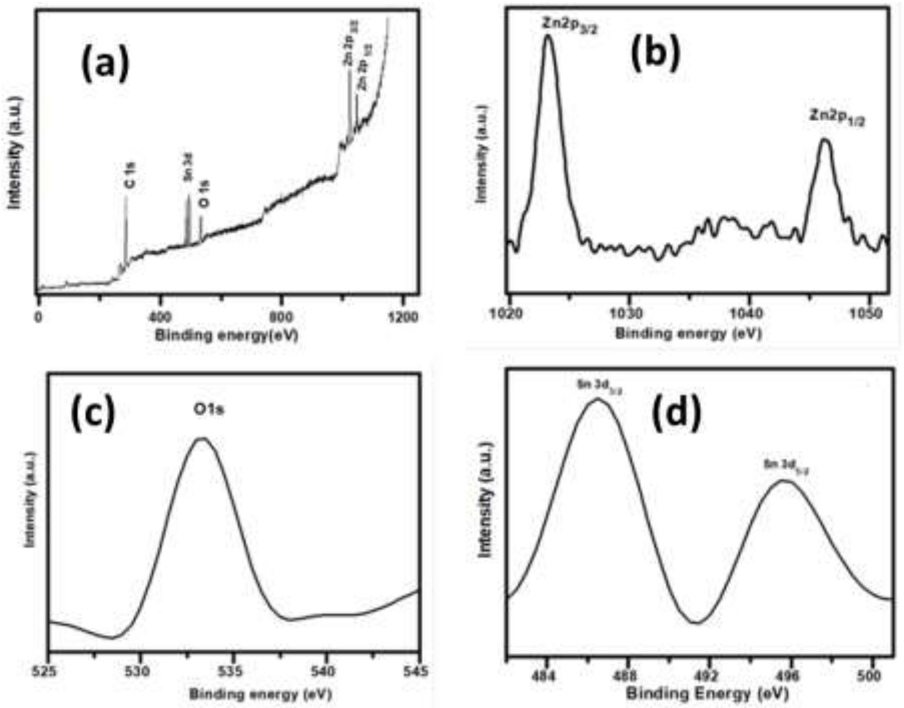

***Figure 4.*** *XPS spectra of Sn-ZnO (a) Survey spectrum (b) Zn2p (c) O1s and (d) Sn3d.*

XPS analysis was performed to identify the elements present in the sample. The survey spectrum for the Sn-ZnO sample is presented in Figure 4(a). The energy scale was calibrated with the C 1s peak at 284.6 eV as reference. The peaks observed at 1023 eV and 1046 eV are assigned to the electronic states of Zn $2P_{3/2}$ and Zn $2P_{1/2}$ respectively and indicating that $Zn^{2+}$ ions are dominant in the sample (Figure 4(b)). Figure 4(c) shows O1s XPS spectrum in which the peak observed at 533 eV is attributed to $O^{2-}$ ions of ZnO. Figure 4(d) shows the Sn 3d spectrum of the sample. There are two main peaks positioned at the binding energy sites of 487eV and 495eV corresponding to the Sn $3d_{5/2}$ and Sn $3d_{3/2}$ orbital respectively and indicating the existence of Sn ions in the sample [41, 42].

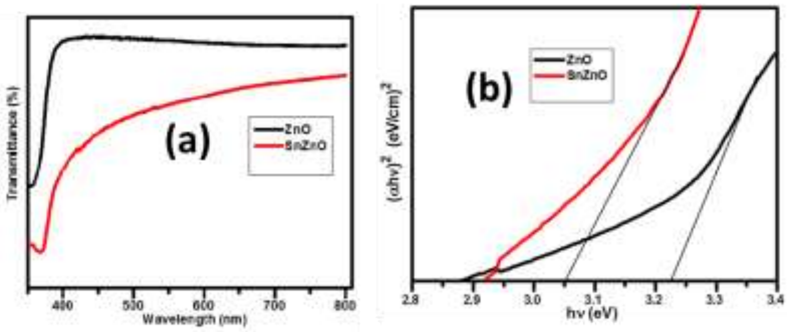

***Figure 5.*** *(a) Optical transmission spectra of Pure and Sn-ZnO and (b) plot of $(\alpha h\nu)^2$ versus Photon energy.*

### 4.3 Optical Studies

The optical transmission spectra of pure and Sn-ZnO samples are shown in Figure 5(a). The samples are transparent in the visible optical region, and with increase in Sn doping, the transmittance maxima decrease. The optical band gap ($E_g$) was estimated from the Tauc's relation [43],

$$(\alpha h\nu)^2 = A\,(h\nu - E_g)$$

where A is an energy dependent constant, $E_g$ is the optical band gap of the sample. The optical band gap energy was calculated by extrapolation of the linear part of plot between $(\alpha h\nu)^2$ and hν as shown in Figure 5(b) and the estimated band gap values are 3.22eV and 3.05eV respectively for pure and Sn-ZnO. Signal at 380nm might be due to charge transfer excitation, the absorption bands resulted from transition $\pi \rightarrow \pi^*$ and $n \rightarrow \pi^*$ involving π orbitals and lone pairs (n=non-bonding). With Sn doping the band gap value of ZnO decreases. This might be due to band gap shrinkage effect by increased carrier concentration [44]. This decrease in the bandgap has two major advantages. Lower band gap facilitates electron excitation with comparatively low energy and hence meets the requirements for visible photocatalysis. Electrons available in the conduction band for the photocatalytic reaction increases and enhances the photodegradation. Further, doping introduces intermediate states within the conduction band and valence band. These intermediate states help in trapping the excited electron that causes enhanced charge separation thereby inhibiting recombination [30].

### 4.4 Studies on Photocatalytic Ozonation

#### 4.4.1 Effect of Ozone Dosage

To find out the optimal ozone dosage required for the degradation of dyes, the ozone dosage was varied from 0 g/h to 0.52 g/h. The removal rate was found to increase linearly with increase in ozone dosage and decreases after 0.48 g/h as shown in Figure 6.

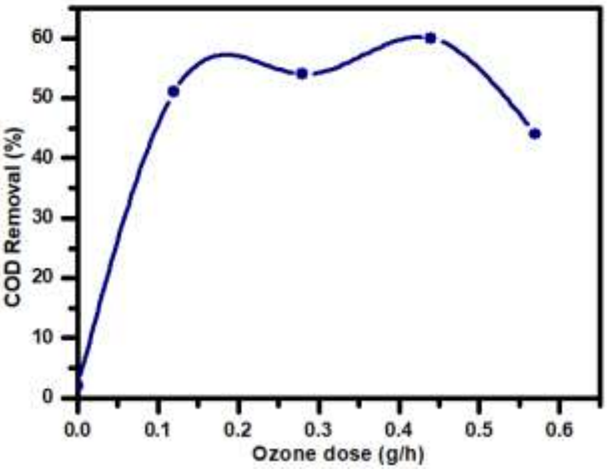

***Figure 6.*** *Effect of Ozone dose on nano-PCO for degradation of azo.*

The COD removal was 61.6% for the mixture of dyes at the end of 60 min. The increased COD removal could be attributed to fast reaction of ozone with reactant molecules. But at very high dosage, some of ozone may escape out without reacting with the pollutant due to less contact time of ozone with the reactant. The additional increase in flow rate of ozone would no longer contribute to increase the removal of the pollutant and hence it is optimized at this point [45]. Similar studies on the Photocatalytic ozonation degradation of textile dye by Cadmium doped ZnO resulted in 88.6% decolourisation [29].

#### 4.4.2 Effect of pH

Ozone can degrade organic pollutants either by direct electrophilic attack at acidic or neutral pH or by indirect attack through the formation of hydroxyl radical at alkaline pH. For the photocatalytic process, generally the pH has varied effect on the process based on the surface adsorption properties. In this study, the reaction was carried out at pH 3, 6 and 9 with 0.2 g/L Sn-ZnO and 0.48 g/h of $O_3$. The COD removal in 180 min was 78%, 82% and 80% at pH 3, 6, and 9 respectively as shown in Figure 7.

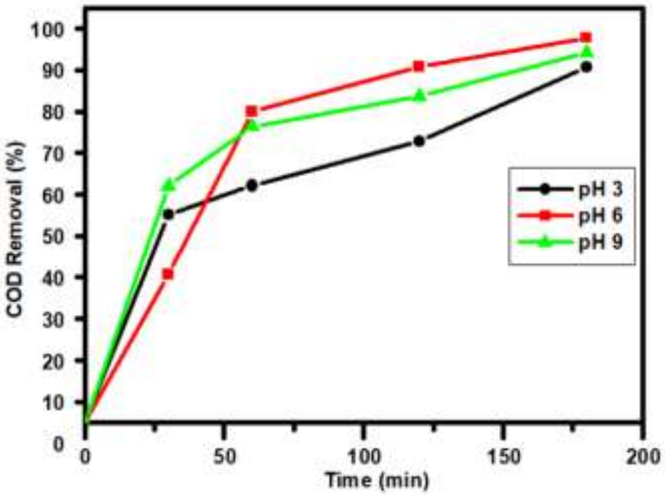

***Figure 7.*** *Effect of pH on nano-PCO for degradation of azo dyes.*

The results indicate at high pH due to faster decomposition of ozone the synergism was lost in PCO and hence neutral pH was suggested for the degradation of dyes [45]. With Copper doped ZnO catalyst used for photocatalytic ozonation of Amaranth [46] also reported that 63.5% degradation with pH 6 whereas with pH 3 and 9 it was respectively 54% and 52%.

### 4.4.3 Effect of Catalyst Dosage

In photocatalytic processes, catalyst dosage is an important parameter. Thus, the influence of initial catalyst on PCO of dyes was examined by using different concentrations of Sn-ZnO ranging from 0 to 1 g/L with 20 mg/L of dyes and 0.48 g/h $O_3$ dosage at pH 6. When the catalyst concentration was increased, an increase in COD removal was observed as shown in Figure 8 and was 68% with 0.2g/L of catalyst.

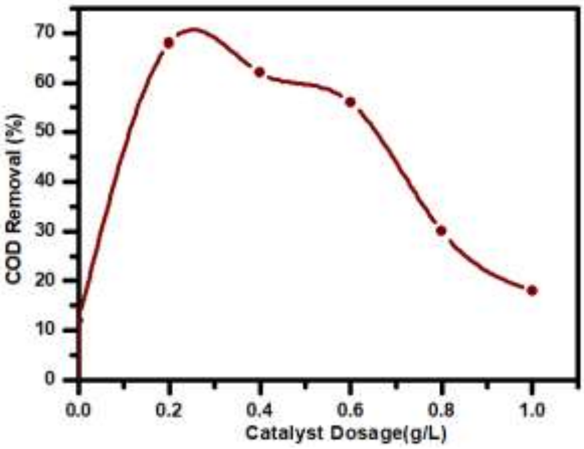

***Figure 8.*** *Effect of Catalyst Dosage on nano-PCO for degradation of azo dyes.*

Nevertheless, a further rise in Sn-ZnO concentration to 1 g/L did not lead to corresponding enhancement in COD removal. The gradual increase in COD removal was attributed due to the fact that with increase in catalyst concentration, the surface area and thus the number of active sites increase. When the catalyst concentration is too high, the excess catalyst might lead to a shielding effect on the penetrating radiation. Penetration of light into reactor is hampered by the increased turbidity of the solution [46].

### 4.4.4 Effect of Dye Concentration

The degradation of dyes at different concentrations (5, 10, 15, 20 and 50 mg/L) for a catalyst loading of 0.2g of Sn-ZnO was investigated and shown in Figure 9. The degradation efficiency was to be inversely proportional to the increase in concentration. Degradation was found to decrease with increase in the concentration of the dye and decolourisation was almost complete even at higher concentration. Also, the graph in Figure 9 shows that even at 50 ppm the degradation efficiency was 45% which means that Sn-ZnO worked well at high concentration. Initially, the catalyst surface area available helped to increase degradation efficiency but with a further increase of dye concentration (at 50 mg/L) active sites of the catalyst were fully occupied by dye molecules and no space was available for $OH^{\bullet}$ radicals' generation.

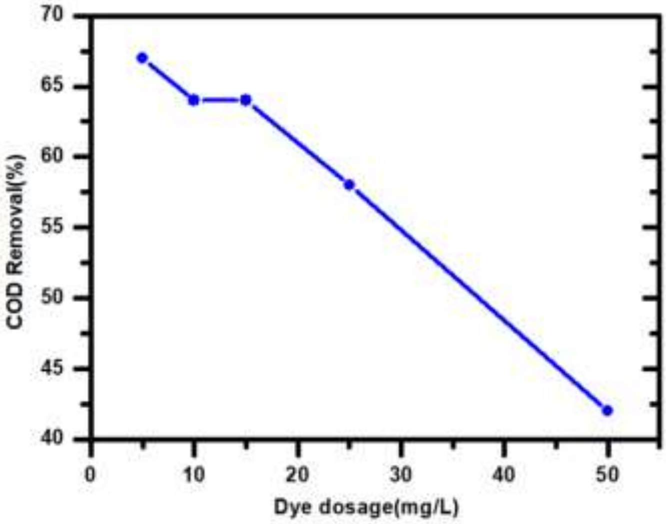

***Figure 9.*** *Effect of Dye Dosage on nano-PCO for degradation of azo dyes.*

The high concentration of dye would have acted as a filter for the incident light, which ultimately reduced degradation efficiency. Similar results have been reported [46] with Amaranth dye degradation by Copper doped ZnO where 98% decolourisation and 68% degradation was achieved with 25 mg/L of dye. But when the dye concentration was increased to 50mg/L, only 28% degradation was noted even though decolourisation around 80%.

### 4.4.5 Mineralisation Studies and Synergistic Effect

The mineralization of mixture of these dyes by the application of different treatment procedures has been studied by the reduction in TOC content. In table 1, TOC removal by different processes is presented. Blank experiments were also carried out to illustrate the effect of light in the absence of catalyst and the effect of catalyst in the dark.

It was obvious from the results that the dyes did not mineralize either by the catalyst alone or by UV radiation alone and indicated that neither hydrolysis nor photolysis had taken during the course of the reaction. 75.4% TOC removal was achieved with nano PCO. The initial rate of dye mineralization by the application of different techniques is obtained from slopes of TOC/TOCo vs. time up to 180 min indicates that degradation rate constant with nano PCO was higher than the individual and other combined AOPs.

It is clearly seen from table 1 that Sn-ZnO/UV/$O_3$ was the most efficient AOP. However, the question arises whether this is just due to two independent AOPs (Sn-ZnO/UV and $O_3$/UV) contributions or due to some synergistic effect of $O_3$ on Sn-ZnO/UV process. In combined nano photocatalytic ozonation process, the rate constant observed was 2.6 times higher than that observed in $TiO_2$ photocatalysis and 2.1 times higher than ozonation process which proves the synergistic effect in the combined process. Three possible reasons for this synergistic effect of $O_3$/UV and Sn-ZnO/UV is[39]:

a) $O_3$ as a stronger oxidant than $O_2$ is more easily reduced by a photogenerated conduction electron from Sn-ZnO producing ozonide radical anion, which in the next step generates hydroxyl radicals (equation 1, 2 and 3).

$$O_3 + e^- \longrightarrow O_3^{\bullet -} \quad (1)$$
$$O_3^{\bullet -} + H^+ \longrightarrow HO_3^{\bullet} \quad (2)$$
$$HO_3^{\bullet} \longrightarrow O_2 + HO^{\bullet} \quad (3)$$

b) Due to more efficient trapping of photogenerated electrons by ozonation the recombination between holes and electrons is minimized. Consequently, a larger number of radicals are produced, thereby accelerating photocatalytic reaction.

c) Even if molecular oxygen accepts the photogenerated electrons a resulting superoxide radical anion can react with ozone to give in subsequent steps a hydroxyl radical (equation 4 - 7).

$$O_2 + e^- \longrightarrow O_2^{\bullet -} \quad (4)$$
$$O_2^{\bullet -} + O_3 \longrightarrow O_3^{\bullet -} + O_2 \quad (5)$$
$$O_3^{\bullet -} + H^+ \longrightarrow HO_3^{\bullet} \quad (6)$$
$$HO_3^{\bullet} \longrightarrow O_2 + HO^{\bullet} \quad (7)$$

Consequently, when the Sn-ZnO is nano photocatalyst is irradiated in the presence of ozone, a greater number of hydroxyl radicals are produced compared to the presence of oxygen. Ozone therefore acts as a powerful oxidant in place of oxygen mainly owing to the fact that ozone is more electrophilic than $O_2$ towards electron photogenerated onto the Sn-ZnO surface. This fact can justify the significant positive effect of nano photocatalysis coupled with ozonation on the degradation of dyes. It is not just the combination of two different processes but the synergistic effect of ozone on nano photocatalyst is clearly shown by the mechanism of nano PCO depicted in Figure 10.

The degradation of different dye samples measured by analyzing the COD content of the wastewater and the results are shown in Figure 11. Comparing to degradation, decolourisation was very much faster and complete decolourisation could be achieved in 45 minutes as shown in Figure 12.

### 4.5 Stability and Reusability Studies

In any treatment methods involving photocatalysts, the life time and the reusability of the catalyst is an important parameter as it determines the cost involved the process [47-49]. Hence, in the present study the stability and reusability of the Sn-ZnO catalyst was studied with PCO process and was evaluated in six successive cycles for the degradation of different dye samples. After each run, the photocatalyst was recovered by centrifugation (4000 rpm for 15min) and redispersed in dye solution without any washing or drying. As shown in Figure 13(a-c), after six cycles, the photocatalytic efficiency decreased slightly compared to the as-synthesized Sn-ZnO for all dyes, thus indicating that the photocatalyst exhibits high stability.

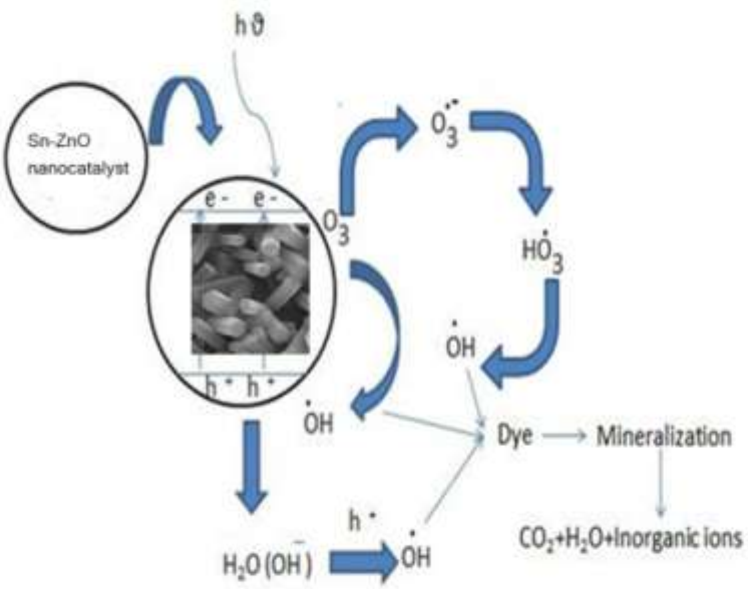

**Figure 10.** *Mechanism for Photocatalytic Ozonation by nano Sn-ZnO/$O_3$/UV.*

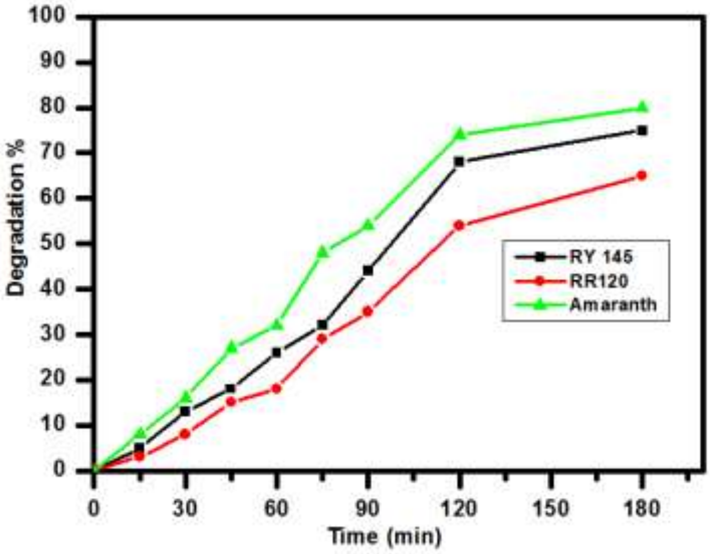

**Figure 11.** *Degradation of Azo dyes by nano Sn-ZnO/$O_3$/UV.*

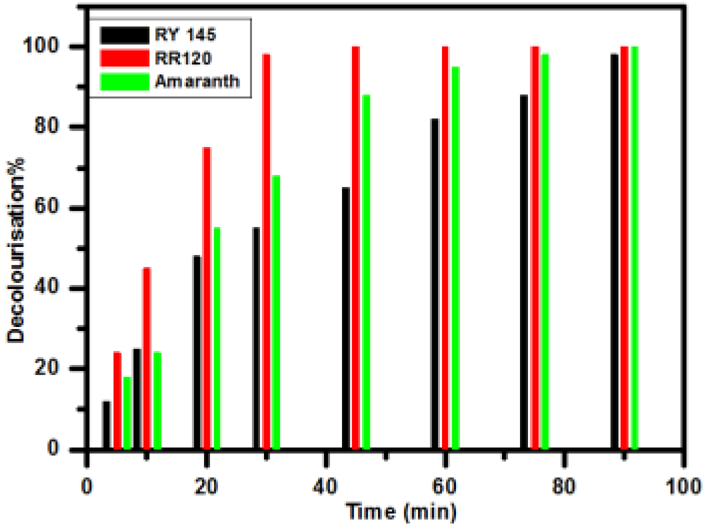

**Figure 12.** *Decolourisation of Azo dyes by nano Sn-ZnO/$O_3$/UV.*

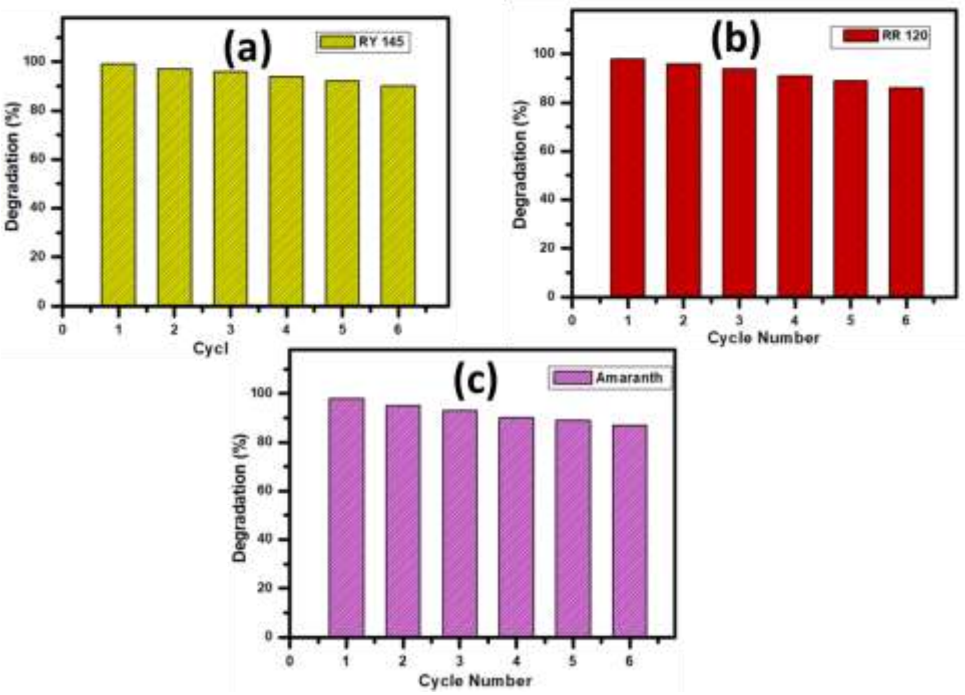

***Figure 13.*** *a, b, c) Plot of photodegradation percent of dyes using the Sn-ZnO catalyst at optimized conditions versus cycle number.*

A study on photocatalytic ozonation degradation of oxytetracycline the stability and reusability of catalyst was acceptable and only 7% decrease in efficiency is reported [50].

## 5. CONCLUSION

Nanorod structured pure and Sn-ZnO samples were prepared by hydrothermal method. The XRD results indicate that the Sn doping does not change the wurtzite structure of ZnO in the sample. EDAX and XPS proves the presence of tin in ZnO. FESEM images showed that the sample consist of hexagonal nanorod morphology without any crack. The band gap determined from optical transmittance spectra shows a reduction in band gap for Sn-ZnO. Prepared nanocatalyst in combination with ozonation under the influence of UV light proved to be a better treatment method for the degradation of dyes. The efficiency and stability of this nano PCO is evaluated with the degradation of different azo dyes and it could possibly be a cost effective simple method for the industries to adopt for the treatment of their complex structured recalcitrant pollutants.

## REFERENCES

1. Saravanan, A., Deivayanai, V. C., Senthil Kumar, P., Gayathri, R., Hemavathy, R. V., Harshana, T., Gayathri, N., Krishanpandi A., “A detailed review on advanced oxidation process in treatment of wastewater: Mechanism, challenges and future outlook”, *Chemosphere*, 308(3) (2022) 136524.
2. Syam Babu, D., Srivastava, V., Nidheesh, P. V., Suresh Kumar, M., “Detoxification of water and wastewater by advanced oxidation processes”, *Science of the Total Environment*, 695 (2019) 133961.
3. Yang, D., Zhao, R., “Advanced Oxidation Processes (AOPs) in wastewater treatment”, *Curr. Pollution Reports*, 1(3) (2015) 167-176.
4. Gogate, P. R., Pandit, A. R., “A review of imperative technologies for wastewater treatment I: oxidation technologies at ambient conditions”, *Adv. Environ. Res.*, 8 (2004a) 501-551.
5. Antonopoulou, M., Evgenidou, E., Lambropoulou, D., Konstantinou, I., “A review on advanced oxidation processes for the removal of taste and odor compounds from aqueous media”, *Water Res.*, 53 (2014) 215-234.

6. Nirmalendu, S. M., Rajesh, R., Aneek, K., Rani, A., Priya, M., Nawaz, A., Saravanan, P., "A Review on Advanced Oxidation Processes for Effective Water Treatment", *Current World Environment*, 12(3) (2017) 470-490.
7. Bilinska, L., Gmurek, M., Ledakowicz, S., "Comparison between simulated textile wastewater treatment by AOPS-Biodegradability, toxicity and cost assessment", *Chemical Engineering Journal*, 306 (2016) 550-559.
8. Shrivani, M., Naji, L., "Effect of seed layer on Morphology of Zinc oxide nanorods as an electron transport layer in polymer solar cells", *International Journal of Nanoscience and Nanotechnology*, 16(3) (2020) 201-208.
9. Divya, B., Karthikeyan, C., Rajasimman, M., "Chemical synthesis of Zinc oxide nanoparticles and its application of dye decolorization", *International Journal of Nanoscience and Nanotechnology*, 14 (2018) 267-275.
10. Raha, S., Ahmaruzzaman, Md., "ZnO nanostructured materials and their potential applications: progress, challenges and perspectives", *Nanoscale Adv.*, 4 (2022) 1868.
11. Baruh, S., Pak, S. K., Dutta, J., "Nanostructured zinc oxide for water treatment", *Nanoscience and Nanotechnology-Asia*, 2 (2012) 90-102.
12. Udo, M. K., Ram, E. K., Stefanakos, A. F., Hepp, D., Yogi, G., "One Dimensional-ZnO Nanostructures: Synthesis, Properties and Environmental Applications", *Mater. Sci. Semicond. Process,* 16 (2013) 2070-2083.
13. Muruganandham, M., Zhang, Y., Suri, R., Lee, G. J., Chen, P. K., Hsieh, S. H., Sillanpaa, M., Wu, J. J., "Environmental applications of ZnO materials (Review)", *Journal of Nanoscience and Nanotechnology*, 15(9) (2015) 6900-6913.
14. Aisah, N., Gustiono, D., Fauzia, V., Sugihartono, I., Nuryadi, R., "Synthesis and enhanced photocatalytic activity of Ce-doped Zinc oxide nanorods by hydrothermal method", *Materials Science and Engineering*, 172 (2017) 012037.
15. Jongnavakit, P., Amornpitoksuk, P., Suwanboon, S., Ndiege, N., "Preparation and photocatalytic activity of Cu-doped ZnO thin films prepared by the sol–gel method", *Appl. Surf. Sci.*, 258 (2012) 8192–8198.
16. Zhao, J., Wang, L., Yan, X. Q., Yang, Y., Lei, Y., Zhou, J., Huang, Y. H., Gu, Y. S., Zhang, Y., "Structure and photocatalytic activity of Ni-doped ZnO nanorods", *Mater. Res. Bull.*, 46 (2011) 1207–1210
17. Gopalakrishnan, R., Muthukumaran, S., "Nanostructure, optical and photoluminescence properties of Zn1−xNixO nanoclusters by co-precipitation method", *J Mater Sci: Mater Electron*, 24(4) (2013) S1069–S1080.
18. Manjula G. Nair, Nirmala, M., Rekha, K., Anukaliani, A., "Structural, optical, photocatalytic and antibacterial activity of ZnO and Co doped ZnO nanoparticles", *Mater. Lett.*, 65 (2011) 1797–1800.
19. Madahi, P., Shahtahmasebi, N, Kompany, A., Mashreghi, M., Bagheri-Mohagheghi, M. M., Hosseini, A., "Deposition and characterization of ZnO:Mg thin films: the study of antibacterial properties", *Phys. Scr.*, 84 (2011) 035801-5.
20. Suwanboon, S., Amornpitoksuk, P., Bangrak, P., Muensit, N., "Structural, optical and antibacterial properties of nanocrystalline $Zn_{1-x}La_xO$ compound semiconductor", *Mater. Sci. Semicond. Process*, 16 (2013) 504–512.
21. Rekha, K., Nirmala, M., Nair, Manjula G., Anukaliani, A., "Structural, optical, photocatalytic and antibacterial activity of zinc oxide and manganese doped zinc oxide nanoparticles", *Physica B*, 405 (2010) 3180–3185.
22. Sonal, S., Kaur, J., Namgyak, T., Sharma, R., "Cu doped ZnO nanoparticles: synthesis, structural and electrical properties", *Physica B: Condensed Matter*, 407 (2012) 1223–1226
23. Milenova, K., Stambolova, I., Blaskkov, V., Eliyas, A., Vassilev, S., Shipochka,M., "The effect of introducing copper dopant on the photocatalytic activity of ZnO nanoparticles", *Journal of the University of Chemical Technology*, 48 (2013) 259–64.
24. Nakata, Y., Okada, T., Maeda, M., "Deposition of ZnO film by pulsed laser deposition at room temperature," *Appl. Surface Sci*, 197 (2002) 368–70
25. Chen, B. J., Sun, X. W., Xu, C. X., Tay, B. K., "Growth and characterization of zinc oxide nano/micro fibres by thermal chemical reactions and vapour transport deposition in air", *Physica. E*, 21 (2004) 103–107
26. Anaraki Firooz, A., Keyhani, M., "The effect of different dopants (Cr, Mn, Fe, Co, Cu and Ni) on photocatalytic properties of ZnO nanostructures", *International Journal of Nanoscience and Nanotechnology*, 16(1) (2020) 59-65.
27. Lee, H. J., Kim, J. H., Park, S. S., Hong, S. S. Lee, G. D., "Degradation kinetics for photocatalytic reaction of methyl orange over Al-doped ZnO nanoparticles", *Journal of Industrial and Engineering Chemistry*, 25 (2015) 199-206.
28. Yarahmadi, M., Maleki-Ghaleh, H., Emami Mehr, M., Dargahi, Z., Rasouli, F., Siadati, M. H., "Synthesis and characterization of Sr-doped ZnO nanoparticles for photocatalytic applications", *Journal of Alloys and Compounds*, 853 (2021) 157000.

29. Pandian, L., Rajasekaran, R., Govindan, P., “Synergistic effect of ozone on cadmium doped zinc oxide nanocatalyst for the degradation of textile dyeing wastewater”, *Mater. Res. Express*, 6 (2019) 085513.
30. Siva, N., Sakthi, D., Ragupathy, S., Arun, V., Kannadasan, N., “Synthesis, structural, optical and photocatalytic behavior of Sn doped ZnO nanoparticles”, *Materials Science and Engineering: B*, 253 (2020) 114497.
31. Sun, J. H., Dong, S. Y., Feng, J. L., Yin, X. J., Zhao, X. C., “Enhanced sunlight photocatalytic performance of Sn-doped ZnO for methylene bluedegradation”, *J. Mol. Catal. A: Chem.*, 335 (2011) 145-150.
32. Gottschalk, C., Libra, J. A., Saupe, A., “*Ozonation of water and waste water: a practical guide to understanding ozone and its applications*”, John Wiley & Sons, (2009).
33. Audenaert, W. T., Vandierendonck, D., Van Hulle, S. W., Nopens, I., “Comparison of ozone and HO induced conversion of effluent organic matter (EfOM) using ozonation and UV/$H_2O_2$ treatment” *Water Res.*, 47(7) 2013, 2387–2398.
34. Li, L., Zhu, W., Chen, L., Zhang, P., Chen, Z., “Photocatalytic ozonation of dibutylphthalate over $TiO_2$ film”, *J. of Photochem. Photobiol. A: Chemistry.*, 175 (2005) 172-177.
35. Addamo, M., Augugliaro, V., Lopez, E. G., Loddo, Marci, G., Palmisano, L., “Oxidation of oxalate ion in aqueous suspensions of $TiO_2$ by photocatalysis and ozonation”, *Catal. Today.*, 107-108 (2005) 612-618.
36. Ilisz, I., Bokro., A., Dombi, A., “$TiO_2$-Based Heterogeneous Photocatalytic Water Treatment combined with Ozonation”, *Ozone: Sci. Engg.*, 26 (2004) 585-594.
37. Biglari, H., Adsharnia, M., Alipour, V., Khosravi, R., Sharafi, K., Mahvi, A. H., “A review and investigation of the effect of nanophotocatalytic ozonation process for phenolic compound removal from real effluent of pulp and paper industry”, *Environ. Sci. Pollut. Res. Int*, 24(4) (2017) 4105-4116.
38. Rajeswari, R., Kanmani, S., “Degradation of Pesticide by Photocatalytic Ozonation process and study of Synergistic effect by Comparison with photocatalysis and UV/ozonation processes”, *Journal of Advanced Oxidation Technologies*, 12(2) (2009) 208-214.
39. Agustina, T. E., Ang, H. M., Vareek, V. K., “A review of synergistic effect of photocatalysis and ozonation on wastewater treatment”, *J. Of Photochem. Photobiol. C: Photochemistry Reviews*, 6 (2005) 264-273.
40. American Public Health Association, “*Standard methods for the examination of water and wastewater*”, 21-st edition, Washington DC, USA, (2005).
41. Chewki, Z., Khalilr, A., Denis, C., Mohamed, A., Saad, H., “Influence of Sn Low Doping on the Morphological, Structural and Optical Properties of ZnO Films Deposited by Sol Gel Dip-Coating”, *Advances in Materials Physics and Chemistry*, 4 (2014) 93-104.
42. Sadia, A., Shaheer Akhtar, M., Hyunt-Kee, S., Young, S. K., Hyung, S. S., “Influence of Sn doping on ZnO nanostructures from nanoparticles to spindle shape and their photoelectrochemical properties for dye sensitized solar cells”, *Chemical Engineering Journal*, 187 (2012)351-356.
43. Tauc, J., Grigorovici, R., Vancu, A., *Phys. Stat. Sol.*, 15 (1966) 627-637.
44. Zegadi, C., Abdelkebir, K., Chaumont, ,D., Adnane, M., Hamzaoui, S., “Influence of Sn low doping on the morphological, structural and optical properties of ZnO films deposited by sol gel dip-coating”, *Adv. Mater. Phys. Chem.*, 4 (2014) 93–104.
45. Cernigoj, U., Stangar, U. L., Trebse, P., “Degradation of neonicotinoid insecticides by different advanced oxidation processes and studying the effect of ozone on $TiO_2$ photocatalysis”, *App. Catal. B: Environmental*, 75 (2007) 231-240.
46. Pandian, L., Rajasekaran, R., Govindan, P., “Synthesis, characterization and application of Cu doped ZnO nanocatalyst for photocatalytic ozonation of textile dye and study of its reusability”, *Mater. Res. Express*, 5 (2018)115505.
47. Subash, B., Krishnakumar, B., Swaminathan, M., Shanthi, M., “Highly Efficient, Solar Active, and Reusable Photocatalyst: Zr-Loaded Ag−ZnO for Reactive Red 120 Dye Degradation with Synergistic Effect and Dye-Sensitized Mechanism”, *Langmuir*, 29 (2013) 939−949
48. Diego, H. Q., Ana, R., Pedro, M. A., Beltran, F. J., Plucinski, P. K., “Enhanced activity and reusability of $TiO_2$ loaded magnetic activated carbon for solar photocatalytic ozonation”, *Applied Catalysis B: Environmental*, 144 (2014) 96-106.
49. Akhmal Saadon, S., Sathishkumar, P., Mohd Yusoff, A. R., Hakim Wirzal, M. D., Rahmalan M. T., Nur, H., “Photocatalytic activity and reusability of ZnO layer synthesised by electrolysis, hydrogen peroxide and heat treatment”, *Environ Technol*, 37(15) (2016) 1875-1882.
50. Mehralipour, J., Darvishali, S., Bagheri, S., Kermani, M., “Photocatalytic ozonation process in oxytetracyline degradation in aqueous solution: composite characterization optimization, energy consumption and by-products”, *Scientific Reports*, 13 (2023) 11113.